# Tunable Bragg reflectors on silicon-on-insulator rib waveguides

**Ivano Giuntoni[1,*], Andrzej Gajda[1], Michael Krause[2], Ralf Steingrüber[3], Jürgen Bruns[1] and Klaus Petermann[1]**

[1]*Technische Universität Berlin, Fachgebiet Hochfrequenztechnik, Einsteinufer 25, 10587 Berlin, Germany*
[2]*Technische Universität Hamburg-Harburg, Optische Kommunikationstechnik, Eißendorfer Str. 40, 21073 Hamburg, Germany*
[3]*Fraunhofer Institut für Nachrichtentechnik, Heinrich-Hertz-Institut, Einsteinufer 37, 10587 Berlin, Germany*
**ivano.giuntoni@tu-berlin.de*

**Abstract:** We present the design, fabrication and characterization of Bragg reflectors on silicon-on-insulator rib waveguides. The fabrication is based on a new double lithographic process, combining electron-beam lithography for the grating and photolithography for the waveguides. This process allows the realization of low loss reflectors, which were fully characterized. The influence of the etching depth and of the waveguide geometry on the reflector performance is considered. We demonstrate a reflectivity larger than 80% over a bandwidth of 0.8 nm with an insertion loss of only 0.5 dB. A thermal tunability of the device is also considered, showing that a shift of the reflected wavelength of 77 pm/K is possible.

©2009 Optical Society of America

**OCIS codes:** (230.1480) Bragg reflectors; (130.3120) Integrated optics devices.

## References and links

1. M. P. Bulk, A. P. Knights, P. E. Jessop, R. Loiacono, G. Z. Mashanovich, G. T. Reed, and R. M. Williams, "Optical Filters Utilizing Ion Implanted Bragg Gratings in SOI Waveguides," Adv. Opt. Technol. **2008**, 276165 (2008).
2. S. Homampour, M. P. Bulk, P. E. Jessop, and A. P. Knights, "Thermal tuning of planar Bragg gratings in silicon-on-insulator rib waveguides," Phys. Status Solidi C **6**, S240–S243 (2009).
3. J. T. Hastings, M. H. Lim, J. G. Goodberlet, and H. I. Smith, "Optical waveguides with apodized sidewall gratings via spatial-phase-locked electron-beam lithography," J. Vac. Sci. Technol. B **20**(6), 2753–2757 (2002).
4. D. Wiesmann, C. David, R. Germann, D. Emi, and G. L. Bona,"Apodized Surface-Corrugated Gratings With Varying Duty Cycles," IEEE Photon. Technol. Lett. **12**(6), 639–641 (2000).
5. S. P. Chan, V. M. N. Passaro, G. Z. Mashanovich, G. Ensell, and G. T. Reed, "Third order Bragg grating filters in small SOI waveguides," J. Europ. Opt. Soc.-Rapid Publications **2**, 07029 (2007).
6. D. J. Moss, V. G. Ta'eed, B. J. Eggleton, D. Freeman, S. Madden, M. Samoc, B. Luther-Davies, S. Janz, and D.-X. Xu, "Bragg gratings in silicon-on-insulator waveguides by focused ion-beam milling," Appl. Phys. Lett. **85**(21), 4860–4862 (2004).
7. P. Heimala, T. Aalto, S. Yliniemi, J. Simonen, M. Kuittinen, J. Turunen, and M. Leppihalme, "Fabrication of Bragg Grating Structures in Silicon," Phys. Scr. **T101**(1), 92–95 (2002).
8. T. E. Murphy, J. T. Hastings, and H. I. Smith, "Fabrication and characterization of narrowband Bragg reflection filters in silicon-on-insulator ridge waveguides," J. Lightwave Technol. **19**(12), 1938–1942 (2001).
9. S. Honda, Z. Wu, J. Matsui, K. Utaka, T. Edura, M. Tokuda, K. Tsutsui, and Y. Wada, "Largely-tunable wideband Bragg gratings fabricated on SOI rib waveguides employed by deep-RIE," Electron. Lett. **43**(11), 630–631 (2007).
10. J. Čtyroký, S. Helfert, R. Pregla, P. Bienstman, R. Baets, R. Ridder, R. Stoffer, G. Klaasse, J. PetráČek, P. Lalanne, J. P. Hugonin, and R. M. LaRue,"Bragg waveguide grating as a 1D photonic band gap structure: COST 268 modelling task," Opt. Quantum Electron. **34**(5-6), 455–470 (2002).
11. I. Giuntoni, M. Krause, H. Renner, J. Bruns, A. Gajda, E. Brinkmeyer, and K. Petermann, "Numerical Survey on Bragg Reflectors in Silicon-on-Insulator Waveguides", in *2008 5th Int. Conf. on Group IV Photonics* (IEEE/LEOS 2008), pp. 285–287.
12. J. Tidmarsh, and J. Drake, "Silicon-on-Insulator Waveguide Bragg Gratings," in *Integrated Photonics Research*, Vol. 4 of OSA Technical Digest (Optical Society of America, 1998), paper ITuH4.
13. G. Cocorullo, F. G. Della Corte, and I. Rendina, "Temperature dependence of the thermo-optic coefficient in crystalline silicon between room temperature and 550 K at the wavelength of 1523 nm," Appl. Phys. Lett. **74**(22), 3338–3340 (1999).

#114653 - $15.00 USD Received 22 Jul 2009; revised 18 Sep 2009; accepted 22 Sep 2009; published 29 Sep 2009

## 1. Introduction

Bragg reflectors on integrated waveguides constitute a key element for the realization of integrated resonators and optical filters for wavelength selection or for dispersion compensation. The reliable integration of such a component on the silicon-on-insulator (SOI) platform is hence an important step for the further development of silicon-based integrated systems.

Different approaches were presented for the realization of Bragg gratings on waveguides. The modulation of the core refractive index was achieved with ion implantation [1,2] or with a periodic corrugation of the waveguide, either on the waveguide sidewalls [3] or on the top surface [4–9]. Both approaches lead to comparable results, even though the latter alternative can be implemented with a less expensive and simpler technology.

In this paper we use an optimized fabrication of Bragg reflectors comprising top corrugated SOI rib waveguides (see Fig. 1), which leads to low additional losses. A reliable modelling method for numerical simulations is applied, providing a design rule. Different Bragg reflectors were fabricated, whose full characterization is presented. We provide information on the transmission and reflection spectra, introduced loss and polarization dependence. Furthermore the effect of different grating depths and waveguide widths were experimentally investigated. Finally the fine tuning of the position of the reflected wavelength exploiting the thermo-optical effect was analyzed.

We make use of rib waveguides with a rib height of $t$ = 1.5 µm. They exhibit lower propagation losses and easier fabrication processes compared to photonic wires, and still permit a relatively high integration level.

## 2. Device modelling

A useful wavelength-selective reflector which should act as a filter is expected to fulfill the following requirements. First, at a desired wavelength the largest possible amount of optical power should be back-reflected. At the same time, every wave propagating at a different wavelength should be transmitted with the lowest possible loss. Furthermore, the reflectivity bandwidth should be kept as narrow as possible, corresponding to a high selectivity.

The numerical description of waveguide Bragg gratings is not a trivial task due to the involvement of higher order modes in both propagation directions. We chose a bidirectional mode expansion (BEP) which combines a high reliability with a relatively low computation complexity if a sufficient number of modes is considered [10].

Two-dimensional simulations of Bragg gratings were performed, i.e. the grating was assumed to be on top of a laterally infinite slab waveguide instead of the laterally finite rib waveguide shown in Fig. 1. We systematically analyzed how the geometrical parameters of the grating influence the fulfillment of the cited conditions [11]. This was accomplished associating the fundamental mode of the slab waveguide with the guided mode of the rib waveguide. All the energy which is coupled (reflected or transmitted) into other modes in the slab-waveguide grating was then considered as loss in the rib-waveguide structure.

Considering SOI as the material system, a thickness of $t$ = 1.5 µm for the silicon guiding layer and $\lambda_B$ = 1550 nm for the reflected wavelength, we fixed the grating period as $\Lambda$ = 225 nm according to the Bragg condition $\Lambda = \lambda_B/2n_{eff}$. During the design of the device we tuned the trench depth $d$ of the grating, the overall length $L$ and the duty cycle $D = a/\Lambda$, defined as the ratio between the width of the grating trenches $a$ and the period $\Lambda$ (See Fig. 1).

It was observed [11] that the best performances can be achieved with gratings exhibiting narrow and shallow etched trenches, i.e. with $d$ < 150 nm and 0.1 < $D$ < 0.4. Figure 2 shows the

#114653 - $15.00 USD Received 22 Jul 2009; revised 18 Sep 2009; accepted 22 Sep 2009; published 29 Sep 2009
(C) 2009 OSA

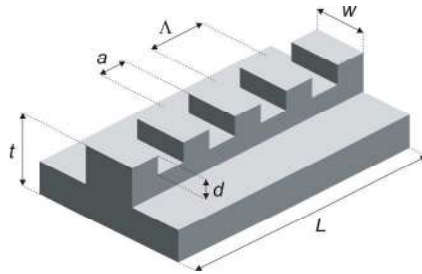


Fig. 1. Geometrical parameters of a silicon-on-insulator rib waveguide Bragg grating: $L$ overall length, $d$ grating depth, $a$ grating trench, Λ grating period, $w$ waveguide width, $t$ rib height, $h$ rib etching depth.

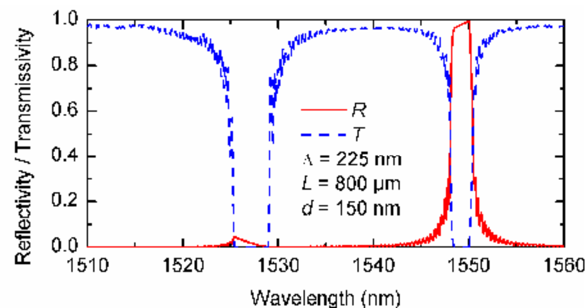


Fig. 2. Calculated reflectivity $R$ and transmissivity $T$ spectra of a Bragg reflector with $d$ = 150 nm, $D$ = 0.3 and $L$ = 800 µm. The grating period is Λ = 225 nm.

simulated spectra of a Bragg reflector in a SOI waveguide that is 800 µm long, 150 nm deep and has a duty cycle of 0.3. At the wavelength 1550 nm a reflectivity of more than 99% is expected, the losses are kept under 0.15 dB outside the reflection bandwidth, which is 2.1 nm broad. At shorter wavelengths around λ = 1525 nm a sudden drop in the transmission curve occurs, this corresponds to a strong coupling to a backward higher order mode.

## 3. Fabrication

The selection of the fabrication process for the designed device was planned with the aim to keep it as simple as possible, avoiding implantation of ions [1,2], ion milling [6] or the deposition of metal layers for the selective masking during the etching steps [8]. The designed Bragg reflectors were fabricated with two separated lithographic processes: a photolithographic one to define the waveguide features and an electron-beam one that defines the gratings on the top of the rib. The two levels of lithography had to be well aligned to each other, to keep the orientation of the grating trenches precisely perpendicular to the waveguides.

Since the quality of the electron-beam lithography is strongly dependent on the morphology of the substrate, the gratings were patterned first on the plain SOI wafer and etched with an inductively coupled plasma (ICP) system using a continuous fluorine-based process and a $SiO_2$ hard mask. After removing the $SiO_2$ hard mask, patterned photoresist was directly used as mask for the etching of the rib waveguide with a reactive ion etching system (RIE), avoiding the deposition of further protection materials. Figure 3 shows an example of the fabricated reflectors. After the processing, the optical facets were polished and covered with an antireflection coating to permit an easier coupling of the light into the waveguides.

All fabricated waveguides exhibit an overall height of t = 1.5 µm, an etching depth of h = 0.7 µm and widths w varying between 1.0 and 2.2 µm. Two different sorts of Bragg reflectors were fabricated, all with an overall length of L = 800 µm and duty cycle of D = 0.3.

#114653 - $15.00 USD Received 22 Jul 2009; revised 18 Sep 2009; accepted 22 Sep 2009; published 29 Sep 2009
(C) 2009 OSA

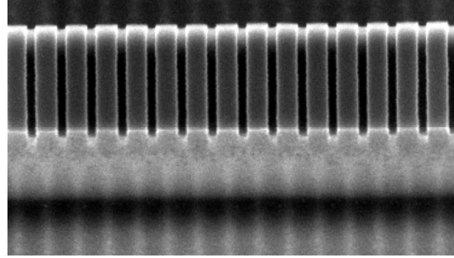

Fig. 3. SEM micrograph with a tilted top view of the fabricated Bragg reflector with an etching depth of 80 nm on a 1.6 µm wide rib waveguide.

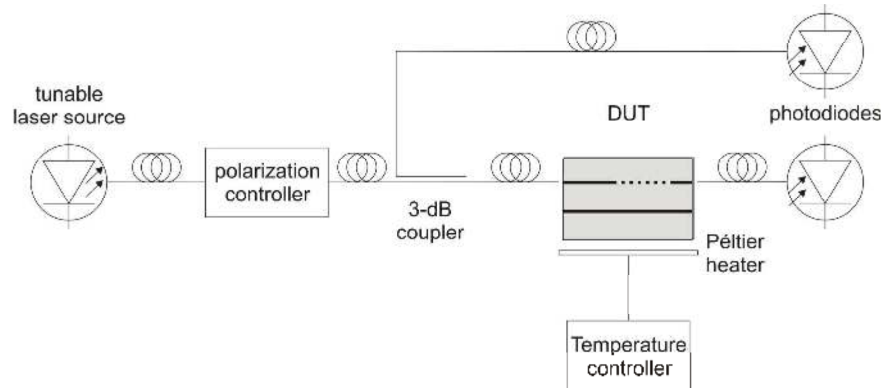


Fig. 4. Scheme of the measurement setup used for the characterization of the fabricated Bragg reflectors.

The first group exhibits a period of Λ = 226 nm and a grating depth of d = 80 nm, the second one a period of Λ = 225 nm and a grating depth of d = 150 nm.

## 4. Measurement results

The measurement setup used for the characterization of the fabricated Bragg reflectors is shown on Fig. 4 and consists basically on a transmission measurement setup, where the single pass transmission through the silicon waveguide is measured. An efficient in- and out-coupling was achieved using lensed fibers, which also allowed to avoid any direct contact with the waveguide facets.

The analysis of the spectral behavior of the fabricated reflectors was performed with a tunable laser source between 1500 and 1600 nm. A polarization controller allowed to set the polarization of the propagating light, while a 3-dB fiber coupler was inserted before the incoupling lensed fiber to separate the signal reflected from the Bragg reflector.

The grating transmissivity was calculated as the ratio between the power transmitted by a waveguide with grating and the one transmitted by a common waveguide.

For the calculation of the reflectivity *R*, as indicated in Eq. (1), we considered the ratio between the power reflected by the grating, compared to one reflected by a straight waveguide, and the input power, estimated by the transmission between the two lensed fibers without any waveguide. Furthermore the effect of the 3-dB coupler, as well as the coupling efficiency and the propagation loss were considered. It follows:

$$R = \frac{P_{grat} - P_{wg}}{P_{in} K \eta^2 \exp(-2\alpha L)} \tag{1}$$

#114653 - $15.00 USD Received 22 Jul 2009; revised 18 Sep 2009; accepted 22 Sep 2009; published 29 Sep 2009
(C) 2009 OSA

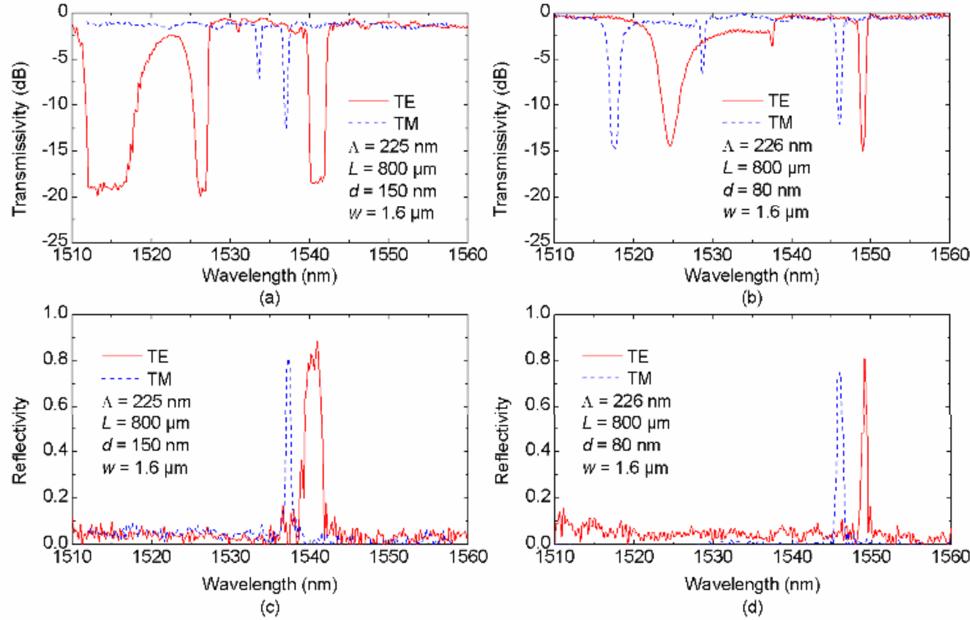


Fig. 5. Transmission and reflection spectra for Bragg reflectors fabricated on a 1.6 µm wide rib waveguide. The grating depth is (a,c) 150 nm and (b,d) 80 nm, the period 225 nm (a,c) 226 nm (b,d) and the length 800 µm.

where $P_{grat}$ is the reflected power measured from a waveguide with grating, $P_{wg}$ the reflected power from a waveguide without grating, $P_{in}$ the estimated input power, $K$ = 0.5 the coupling ratio of the external 3-dB fiber coupler, η the coupling efficiency into the waveguide (0.47 estimated with a virtual cut-back measurement of straight waveguides exhibiting different lengths), α the linear propagation loss coefficient of the waveguide (0.2 dB/cm measured on a parallel straight waveguide) and $L$ the distance between the incoupling facet and the Bragg grating. In Eq. (1) the effect of the resonator created between the reflector and the facet is neglected, because of the propagation loss in the rib waveguide and the presence of the antireflection coating.

In Fig. 5 the measured spectra for Bragg reflectors with two different etching depths are shown. It can be observed that shallow etched gratings (right-hand spectra in Fig. 5) introduce a low loss, in the order of 0.5 dB. At the Bragg wavelength a reflectivity of 80% is achieved over a narrow bandwidth of 0.8 nm for the TE polarization, corresponding to an extinction ratio of 15 dB in the transmission. At shorter wavelengths, around 1525 nm, a broad drop in the transmission spectrum is present, corresponding to a coupling to backward higher order modes, as already observed in the simulations (see Fig. 2). Since they cannot be guided in a single-mode rib waveguide, they are not back reflected and leak out. This is confirmed by the absence of any reflected signal at these wavelengths. Increasing the grating depth (left-hand spectra in Fig. 5), a stronger effect on the TE mode can be observed, with a larger extinction ratio up to 19 dB and a broadening of the reflection bandwidth to 2.1 nm. The device can still be considered transparent outside the reflection bandwidth, since the introduced loss is kept below 1 dB. Deeper etched trenches on the waveguide rib also enhance the coupling to leaky modes at shorter wavelengths, as it can be seen on the transmission spectra. A peak of 88% of reflected power was measured for the TE mode.

For both etching depths the reflected wavelength for the TM mode is shifted by 3 nm towards shorter wavelengths in respect to the TE reflection peak, indicating a waveguide birefringence of 7 x $10^{-3}$. Furthermore deeper etched grating trenches introduce no evident change on the TM behavior: peak reflectivity, bandwidth and extinction ratio remain comparable to the ones obtained from shallower gratings. This would suggest that the

#114653 - $15.00 USD Received 22 Jul 2009; revised 18 Sep 2009; accepted 22 Sep 2009; published 29 Sep 2009
(C) 2009 OSA

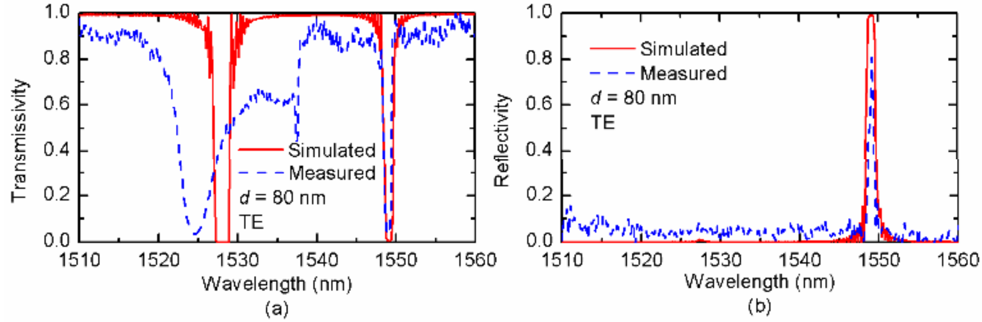


Fig. 6. Comparison between computed and experimentally measured (a) transmission and (b) reflection spectra. The grating depth is $d = 80$ nm, the period $\Lambda = 226$ nm and the overall length $L = 800$ µm. TE polarization is considered. All spectra are in linear scale.

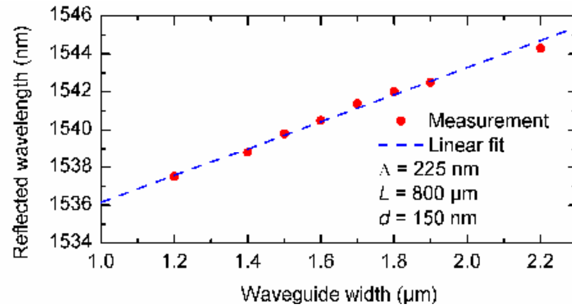


Fig. 7. Dependence between the peak reflected wavelength and the width of the waveguide. The points represent the measured data, the dashed line is a linear fit.

interaction between the TM optical field and the grating etched on the top of the waveguide rib is relatively weak compared to the TE polarization.

The comparison between the numerically computed and the measured spectra of the TE mode for the shallow etched grating are shown in Fig. 6. It can be observed that around the Bragg wavelength at $\lambda = 1549$ nm the curves are in good agreement with each other. At shorter wavelengths the difference in the curve shape for the transmission spectrum is related to the nature of the modes involved: in the two-dimensional waveguide considered in the simulation the grating couples energy between the forward propagating fundamental mode and a guided higher-order mode, while in the three-dimensional single-mode waveguide this coupling can occur only to leaky and radiating modes. The slightly higher overall loss in the measured transmission spectrum can be related to a possible sidewall roughness of the waveguide, not considered in a two-dimensional calculation.

On Fig. 7 the influence of the waveguide geometry is considered. The measured Bragg wavelength for the TE polarization is depicted as function of the rib width. It can be observed that equal Bragg reflectors fabricated on smaller waveguides exhibit reflection at shorter wavelengths because of the lower effective refractive index.

Choosing the proper combination of waveguide geometry and grating period it is hence possible to design a Bragg reflector for every arbitrary wavelength within the C-band. Once the designed reflector is fabricated, the possibility to dynamically tune the reflected wavelength is strongly desirable. This can be easily achieved varying the operating temperature of the component [2,12]. An increase of the temperature produces two separate effects: first of all a volume dilatation, leading to an expansion of the grating period:

$$\Lambda(T) = \Lambda_0 \left(1 + \gamma \Delta T\right) \tag{2}$$

#114653 - $15.00 USD Received 22 Jul 2009; revised 18 Sep 2009; accepted 22 Sep 2009; published 29 Sep 2009
(C) 2009 OSA

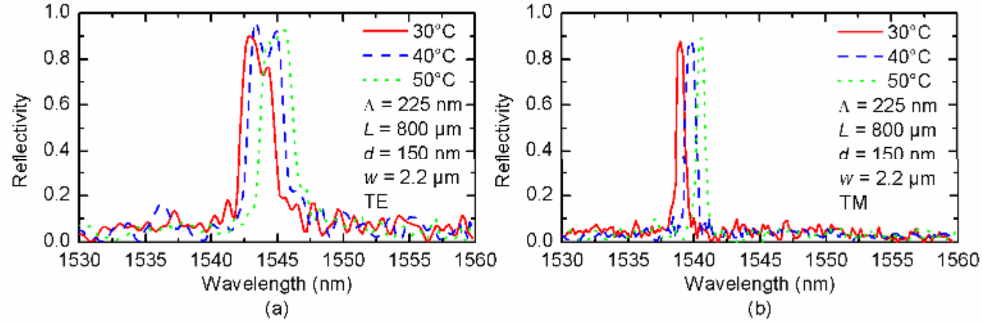


Fig. 8. Reflection spectra a Bragg reflector on a 2.2 µm wide rib waveguide for three different temperatures for both TE and TM polarization. The grating depth is 150 nm, the duty cycle 0.3 and the overall length 800 µm.

and an increase of the material refractive index due to the thermo-optical effect:

$$n(T) = n_0 + \frac{dn}{dT}\Delta T\,. \tag{3}$$

Combining Eq. (2) and (3), the overall thermally induced wavelength shift is hence:

$$\frac{d\lambda}{dT} = 2n_0\gamma\Lambda_0 + 2\Lambda_0\frac{dn}{dT}. \tag{4}$$

Considering silicon as guiding material, the thermal expansion coefficient is $\gamma = 2.5\text{x}10^{-6}$ $K^{-1}$ and the thermo-optical effect around the room temperature is $dn/dT = 1.8\text{x}10^{-4}\ K^{-1}$ [13]. Hence the expected thermally-induced variation of the reflected wavelength of the grating is 80 pm/K. The major contribution in Eq. (4) is given by the thermo-optical effect.

The operating temperature of the fabricated reflectors was modified, mounting them on a Péltier heater. On Fig. 8 the measured reflection spectra for three different temperatures for both polarizations are shown. The expected behaviour can be easily observed, with an evident shift of the reflected wavelength to longer values for higher temperatures. This shift is equal for both polarizations and is around 77 pm/K, which is in good agreement with the theoretically expected value of 80 pm/K and with the one presented in [2].

## 5. Conclusions

We reported the realization and characterization of Bragg reflectors on silicon-on-insulator rib waveguides. We optimized the design of the device to achieve a high reflectivity on a narrow bandwidth and low insertion losses. The fabrication was performed with a simple two level lithographic process, which allows to easily integrate the Bragg gratings with other devices. The measured transmission and reflection spectra of the obtained Bragg reflectors showed that a selective reflection larger than 80% on a bandwidth of 0.8 nm can be achieved, while for other wavelengths the device is transparent, introducing a loss of only 0.5 dB. The narrow bandwidth combined with the possibility to tune the reflection wavelength with the waveguide geometry, makes the device interesting for WDM applications. The dynamic tuning of the Bragg reflector varying the operating temperature was shown, demonstrating a variation of the reflection peak of 77 pm/K.

## Acknowledgments

The financial support of the German Research Foundation (DFG) in the frame of grant FOR653 is gratefully acknowledged.

#114653 - $15.00 USD Received 22 Jul 2009; revised 18 Sep 2009; accepted 22 Sep 2009; published 29 Sep 2009
(C) 2009 OSA